Synthesis and Kinetic Analysis of HCV NS3/4a Protease Inhibitors

Submitted to Worcester Polytechnic Institute for partial fulfillment
of the requirements for the Degree of Bachelor of Science

By: Wasih Kamran

April 27, 2017

Advisors:

Dr. Destin Heilman (WPI)

Dr. Akbar Ali (UMass Medical School)

1 CONTENTS

Acknowledgments

I would like to thank Celia Schiffer for allowing me to conduct this research in her lab. I would also like to thank Akbar Ali and Ashley Matthew from the Schiffer Lab for their constant support and assistance during the entirety of the project. I also wanted to thank Professor Destin Heilman for his guidance when it came to writing this project. Finally, I would like to thank Jacqueto Zephyr, Linah Rusere, and the entire Schiffer Lab for being so kind and accommodating throughout the year and for helping me adapt to working in the Lab.

Abstract

Hepatitis C virus (HCV) is the leading cause of chronic liver cirrhosis and liver cancer in the world. To make more effective antiviral therapies, companies started to develop direct acting antiviral (DAA) drugs that could target specific components of the virus. One therapeutic target for the virus is the NS3/4a protease, which is a vital component in the viral replication cycle. Protease inhibitors (PIs) have been developed, but are susceptible to drug-resistant mutations. This goal of the project was to develop novel PIs based on the potent drug Grazoprevir (MK-5172) and test their inhibition on both the wild type and mutant proteases. Three PIs were synthesized with P1P3 macrocycles and extended P4 residues with P5 capping groups. These inhibitors were analyzed with *in vitro* enzyme inhibition assays against both the wild-type protease and D168A, a common drug resistant mutant. No novel inhibitor was found to be more potent than MK-5172, however one inhibitor (WK-27) was found to have very similar K_i values for both constructs tested and had a flatter resistance profile than MK-5172. Further studying WK-27 can lead to more refined drug design that takes advantage of an extended P4 residue with a P5 capping group.

2 INTRODUCTION

2.1 EPIDEMIOLOGY

Hepatitis C virus (HCV) infection has a global prevalence upwards of 150 million cases and is the leading cause of chronic cirrhosis, liver cancer, and liver transplantation in the world.[1, 2] The main causes of transmission in developed countries like the United States are from blood transfusion and unsanitary injectable drug use, where the incidence rate is less than 2%.[1] In high prevalence areas like Egypt (up to 20% incidence estimated) the main risk factors include unsafe therapeutic injections and unsafe blood transfusion screening practices due to limited resources.[1]

Patients infected with HCV can be asymptomatic for decades, however severe chronic liver symptoms can occur within 20-30 years.[3] A majority (70-80%) of HCV infected patients in the US are in the baby boomer population (50-70 years old), of which 20% exhibit symptoms of advanced liver disease. Of this group, around 70,000 people suffer from decompensated cirrhosis, which typically leads to the patient needing a liver transplant.[3, 4] It is also estimated that 59% of people infected with HCV were undiagnosed in 2008, so it is imperative to limit the burden on the healthcare system by investing in efficient testing and high-efficacy treatment for HCV infected people as the baby-boomer population ages. [3]

2.2 HCV REPLICATION CYCLE

HCV is thought to enter the cell through receptor-mediated endocytosis.[2] After the viral particle enters the cell, the RNA genome is released and translated in the rough ER.[2] The corresponding viral polyprotein (Figure 1b) is cleaved by a variety of host and viral proteases. The structural proteins are cleaved by the host's signal peptidase, while the downstream

nonstructural proteins are cleaved by the NS2 cysteine protease and the NS3-4A serine protease.[5] The NS5A RNA replication assembly protein along with the NS5B RNA dependent RNA polymerase create a negative sense RNA intermediate that is used to create positive-sense RNA progeny that can either be incorporated into viral particles or be used to translate more polyproteins. If they integrate into the viral particle, it is believed that they exit through the secretory pathway.[2]

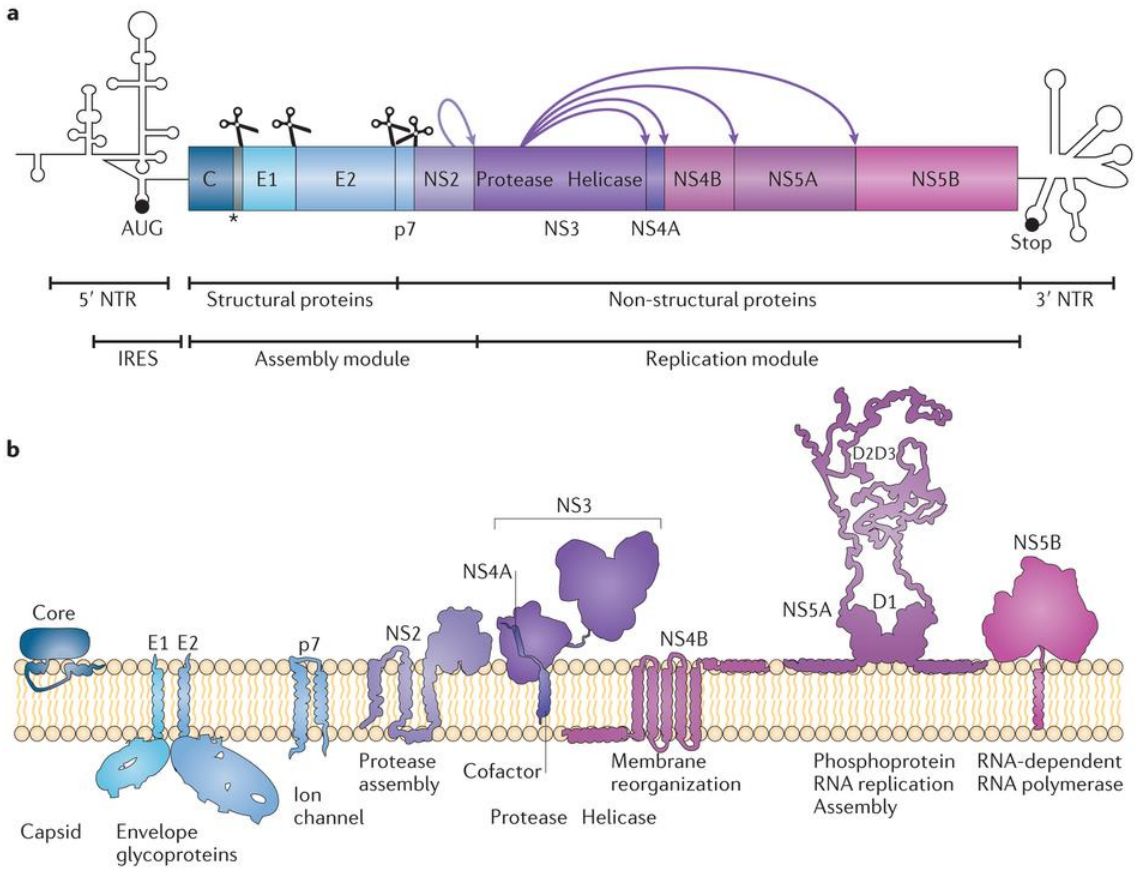

Figure 1-A) Open reading frame of the viral genome. Scissors denote host protease cleavage sites, arrows denote cleavage via viral proteases. **B**) Membrane Topology of viral prteins and their given functions. (Adopted from Bartenschalger et al. (2013).

2.3 HCV GENETICS

As mentioned above, HCV has a single stranded, positive sense genome that encodes for 10 different structural and nonstructural proteins (Figure 1a).[2] The HCV genome is highly variable in sub-species with 6 main genotypes (1-6) and numerous sub-types.[6] The HCV genotypes are uniquely distributed in the global population. For example, genotypes 1a and 1b disproportionately affect higher income regions compared to lower income areas, which are more susceptible to genotype 3 and 4.[3]

2.4 INTERFERON TREATMENT

Before therapeutic strategies can be covered, it is important to outline the parameter used for therapeutic success: sustained virologic response (SVR). SVR indicates no HCV RNA in a patient's serum taken 6 months after the end of treatment (EOT).[5]

The first FDA approved treatment for HCV patients was interferon-α (IFNα) in 1986. IFN is an intracellular signaling protein that has antiviral properties by increasing host natural killer cell activity and maturation.[3, 6] High dose IFNα had 10-20% SVR in HCV patients but came with a myriad of adverse side effects including diabetes mellitus, thyroid disorders and various autoimmune conditions that caused cessation of treatment.[3, 7]

After the low reported SVR of IFNα alone, ribavirin (RBV) was approved for treatment alongside IFNα in 1996.[7] Ribavirin is a purine nucleoside analogue that when combined with IFNα can lead to an SVR of up to 40 %.[3, 8, 9] While the mechanism behind RBV's efficacy with HCV patients is not exactly clear, studies suggest it inhibits viral RNA polymerases and it is

proposed that it acts as a lethal mutagen like it has been proven to do with many other RNA viruses.[8, 9]

Aside from the aforementioned side effects of IFNα, one of the problems with treatment was that it had to be administered subcutaneously three times per week.[11] In order to develop a better dosing procedure and increase drug efficacy, researchers added 12kDa of polyethylene glycol (through a process called PEGylation) to interferon to increase its stability in the body. This PEG-interferon (Peg-IFN) has proven to have a 10-fold greater half-life in the body than regular interferon and an overall increase in patient SVR by 7% when only treated with IFN.[11,12] When combined with ribavirin, the difference in SVR between PEGylated and regular IFN is 7% overall and a 9% increase in SVR among GT-1 patients.[12] While this advancement was encouraging in the treatment of HCV, studies have shown that the regimen achieves 80% SVR in genotype 2 and 3 patients while only achieving 40-50% SVR in genotype 1 patients.[13] Further developments in treatment are now moving past using Peg-IFN/RBV in favor of all oral dosing of direct acting antivirals (DAAs) that will not require difficult dosing procedures or subject the patients to intolerable side effects.[14]

2.5 NS3/4A PROTEASE INHIBITORS

One class of DAAs that have been thoroughly studied are NS3/4a protease inhibitors (PIs). As mentioned in section 1.2, the NS3/4a protease (figure 3) is essential to viral maturation through its involvement in cleaving the viral polyprotein, which makes it an ideal therapeutic target.[14]

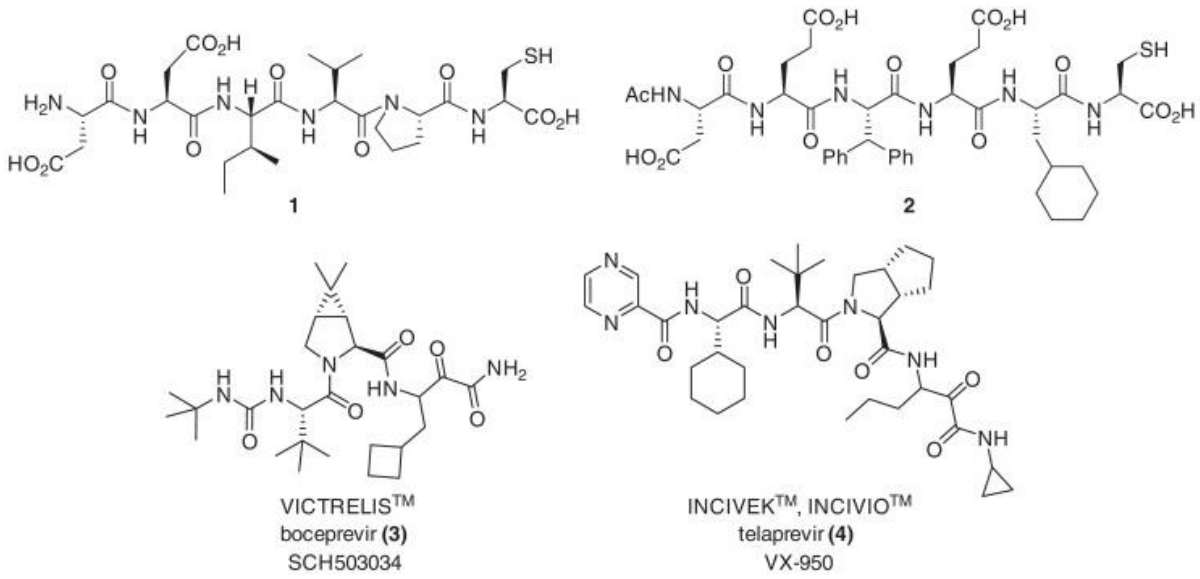

Figure **2:** (**1**) DDICPC-OH cleavage product (**2**) Ac-DEMEEC-OH cleavage product (**3**) boceprevir (FDA approved 2013) **(4)** telaprevir (FDA approved 2011). Adopted from McCauley and Rudd, (2016).

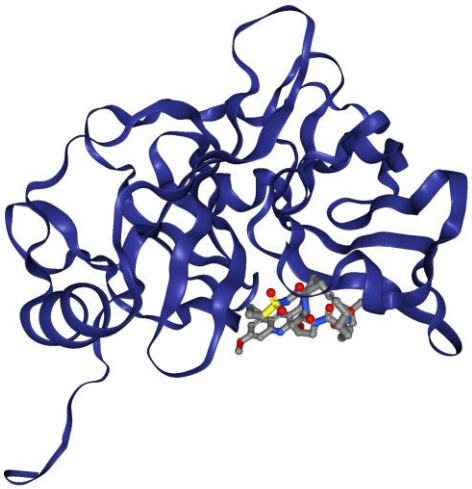

Figure **3**: Crystal structure of HCV NS3/4a protease in complex with P1P3 macrocyclic analogue of Grazoprevir (MK-5172). PDB ID: 5EPN

The first inhibitor for the protease was identified by Boehringer-Ingelheim (BI) and was a product of substrate cleavage that was a hexapeptide (DDIVPC-OH, figure 2).[14] The researchers at BI also found that the product of the NS3 protease's cleavage of the NS4a-4b peptide also

yielded a hexapeptide (Ac-DEMEEC-OH) that had a Ki of 0.6 µM.[14] As structural and kinetic studies continued using these hexa-peptide leads, structural features were added and assessed for biochemical and clinical efficacy. The first breakthrough feature was developed by Boehringer-Ingelheim and involved a macrocycle between the P1 and P3 residues to increase conformational rigidity in the molecule. While early clinical trials for the drug named ciluprevir (BILN-2061) were positive, rhesus safety studies indicated severe cardio-vascular side-effects so the development was discontinued.[14]

In parallel, building off of the hexamer peptide competitive inhibitors, the first two direct acting antivirals that gained FDA approval: telaprevir and boceprevir (approved 2011 and 2013 respectively) were developed.[3, 13, 14]

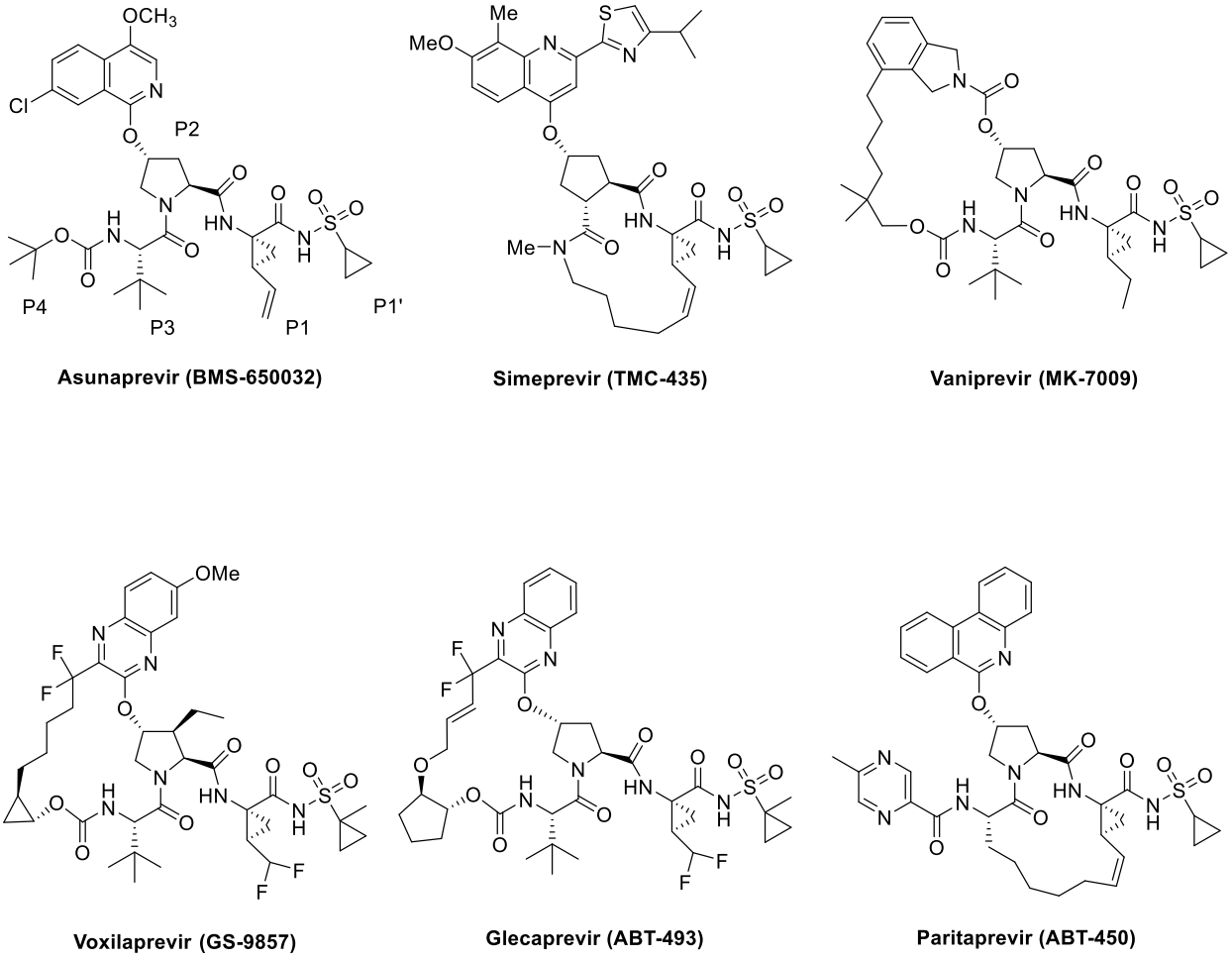

Figure **4:** Chemical structures of clinically relevant PIs. Asunaprevir and Simeprevir are both approved in Japan. Vaniprevir, Voxilaprevir, Glecaprevir and Paritaprevir are all approved in the United States.

While Boehringer-Ingelheim focused on P1-P3 macrocycles, Merck developed a series of P2-P4 macrocyclic compounds starting with vaniprevir (figure 4), which was part of the first treatment regimen to achieve full SVR in an all-oral treatment of primates.[14] The drug was approved for use in Japan with Peg-IFN and RBV. This drug reached sub-nM Ki values in vitro for genotype 1 (GT1) proteases, however it was relatively ineffective in genotype 3 (GT3) and various GT1 mutations.[15] A Ki value of less than 1 nM is indicative of very favorable kinetic inhibition in *in-vitro* assays. The prevalence of drug resistance in many patients being treated with vaniprevir and other PIs led companies to explore further structural changes to their drugs to combat drug resistant mutations.[14]

2.6 GENETIC INFLUENCES ON DRUG RESISTANCE IN HCV TREATMENTS

The general method in which viruses mutate to gain resistance to DAAs is through their highly error-prone RNA dependent RNA polymerases. In HCV, the error-prone NS5B polymerase leads to numerous different mutant "quasispecies" that can exist within the patient alongside the predominant wild-type genotype. These species have been rarely seen in patients that do not receive DAA treatment, however if a patient receives treatment, these quasispecies can arise and thrive if the mutations are present in their target gene, such as NS3/4a protease, NS5A, etc., and have an effect on inhibitor binding, as they will have better selective fitness.[16] Some very common PI resistant mutations in GT1 HCV are R155K, A156T, A156V, and D168A.[15] In biochemical studies, these mutations were found to reduce the efficacy of vaniprevir by at least 100-fold.[15] This reduced protease inhibition drove Merck to develop Grazoprevir (MK-5172), an inhibitor with more broad effectiveness against different mutations and GT3

proteases.[14] When compared to vaniprevir, MK-5172 was far less susceptible to drug resistant mutations D168A and R155K, with small changes of efficacy compared to wild-type protease.[17]

2.7 MOLECULAR STRUCTURE AND DRUG RESISTANCE

To examine the structural basis of PI binding with the protease, Romano et al. (2012) created surface representations using the protease crystal structure in complex with MK-5172 and earlier PIs (figure 5). 3 common interactions were found in all PIs: First, the P1 amide nitrogen forms a hydrogen bond with the carbonyl oxygen of R155. Second, the P3 carbonyl oxygen forms a hydrogen bond with the amide nitrogen of A157. Finally, the P3 amide nitrogen

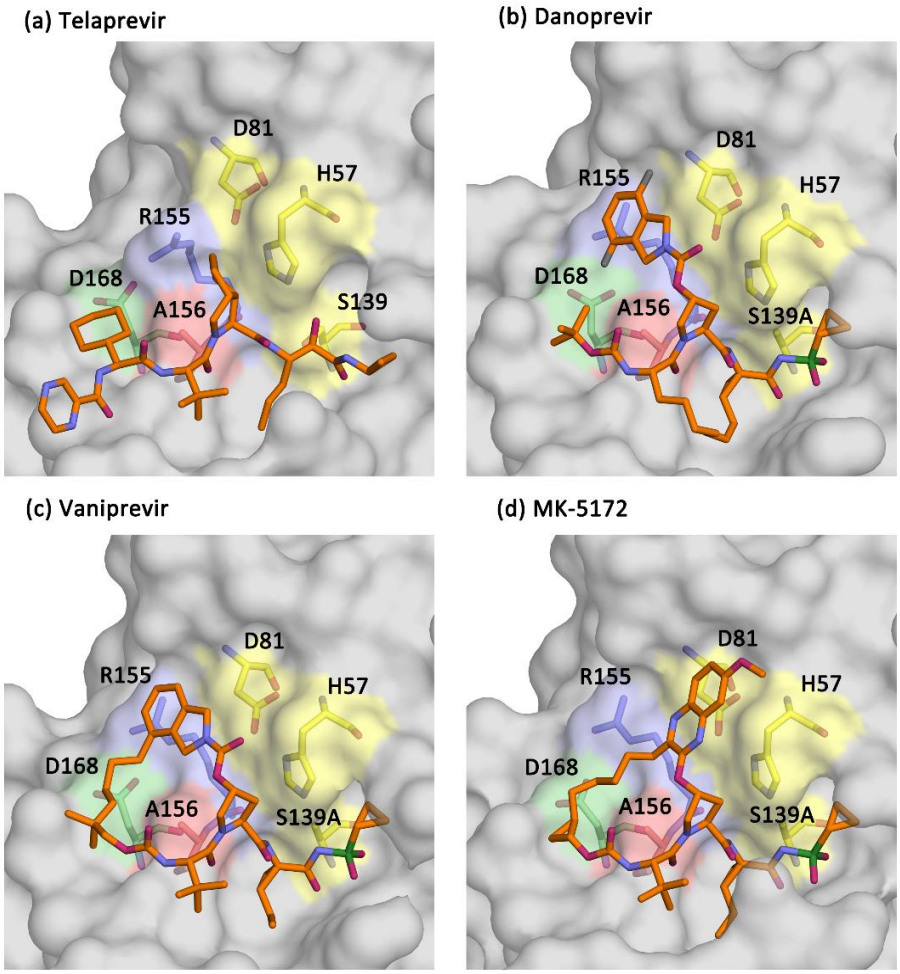

Figure **5**- Surface representations of PI binding: (**a**) Telaprevir, (**b**) Danoprevir, a P1-P3 macrocyclic PI. (**c**) Vaniprevir and (**d**) MK-5172/grazoprevir. Yellow indicates conserved catalytic residues, blue indicates R155, red indicates A156 and green indicates D168. Figures from Romano et al. (2012)

forms a hydrogen bond with the carbonyl oxygen of A157.[17]

When comparing the binding of the four aforementioned PIs to the enzyme's natural substrates, using the substrate envelope of the protease can help elucidate residues of the protease that can confer drug resistance. The substrate envelope is the consensus volume of the substrates that bind with the NS3/4a protease.[17] Figure 6 shows MK-5172 binding to the wild-type protease with the substrate envelope in blue. Areas where the PI protrudes out of the substrate envelope are most likely to be places where mutations can lead to drug resistance. MK-5172, as with the other four drugs listed above, protrudes out of the substrate envelope near residues R155, A156, and D168. Consequentially, mutations in any of the three residues result in multi-drug resistant protease variants.

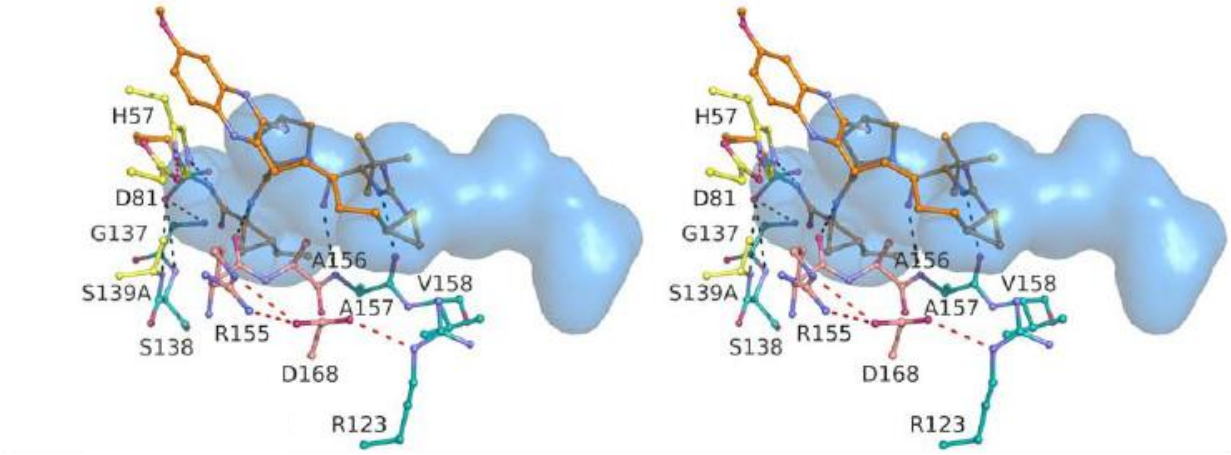

Figure **6:** MK-5172 (orange) and substrate envelope (blue) of wild-type protease, adopted from Romano et al. (2012).

While MK-5172 does protrude out of the substrate envelope at the P-2 quinoxaline, the ring system does not stack with R155 or interact with D168 or adjacent residues.[17] Because of this, there were only small changes to MK-5172's Ki values against R155K and D168A mutants. When looking at the stereo view of MK-5172 with the A156T mutant, a clear steric clash between the P2-P4 macrocycle can be seen (figure 7). Consequentially, MK-5172 had a 1000 fold decrease in potency against A156T.[17]

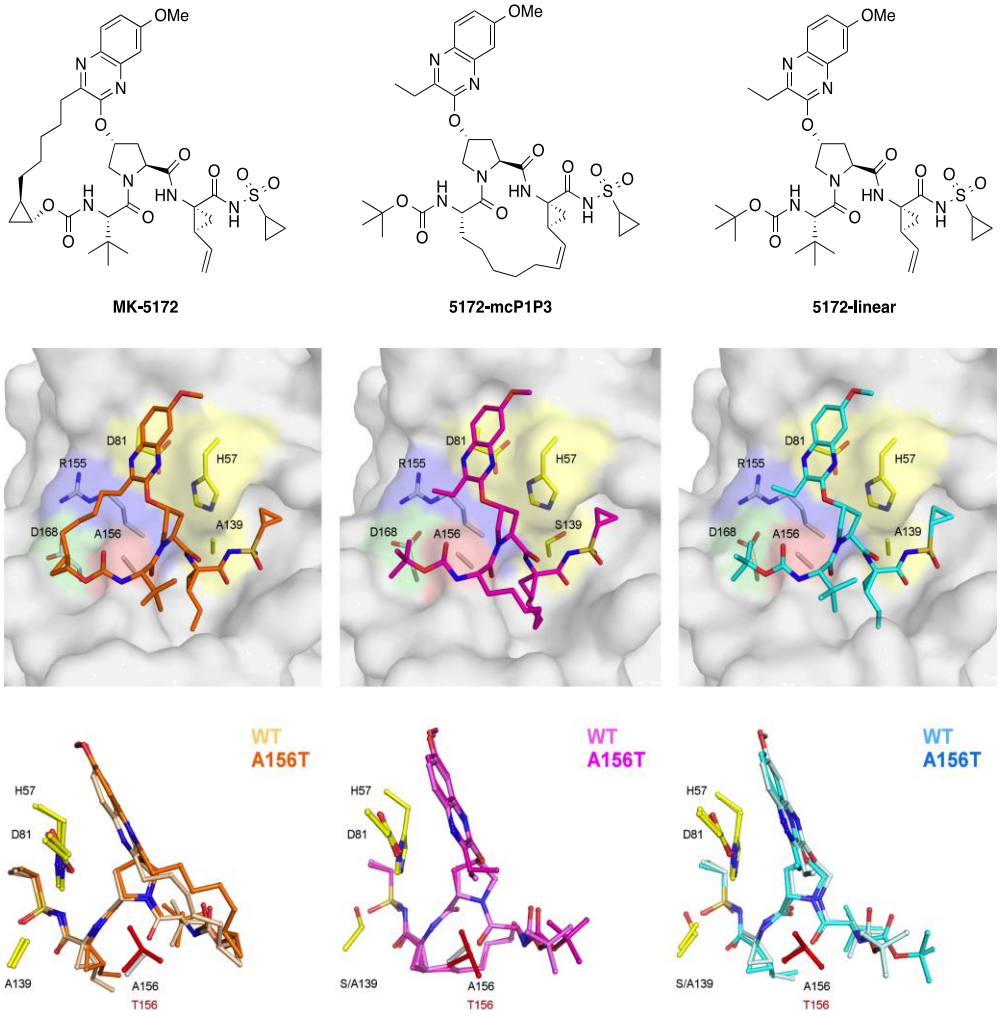

Figure 7: Top: MK-5172, its P1P3 macrocyclic and linear analogue structures. Middle: surface representation of PIs binding with GT-1a protease. Bottom: Conformational changes with A156T mutation.

In order to avoid this steric clash, P1-P3 macrocyclic and linear analogoues of MK-5172 were synthesized and their binding interaction were studied. Surface views of the of the WT NS3/4a protease and A156T mutant in complex with MK-5172 and its analogues are shown in figure 9. When comparing the binding mode of the three inhibitors with the wild-type proteasse, the key areas where the quinoxaline moeity interacts with D81 is maintained regardelss of the macrocycle being present.[18] The main difference is when the A156T mutant bind with the inhibitors. As stated before, there is a steric clash between the A156T residue and the P2-P4 macrocycle of MK-5172, causing the entire inhibitor to change drastically change conformation due to the rigidity of the macrocycle. Both the P1-P3 and linear analogoues can accomdate the added steric bulk of the threonine mutation without a drastic change in overall inhibitor binding to the rest of the protease.[18] The added flexibility of the P1-P3 macrocycle and retained molecular binding made it a suitable molecule to continue to study.

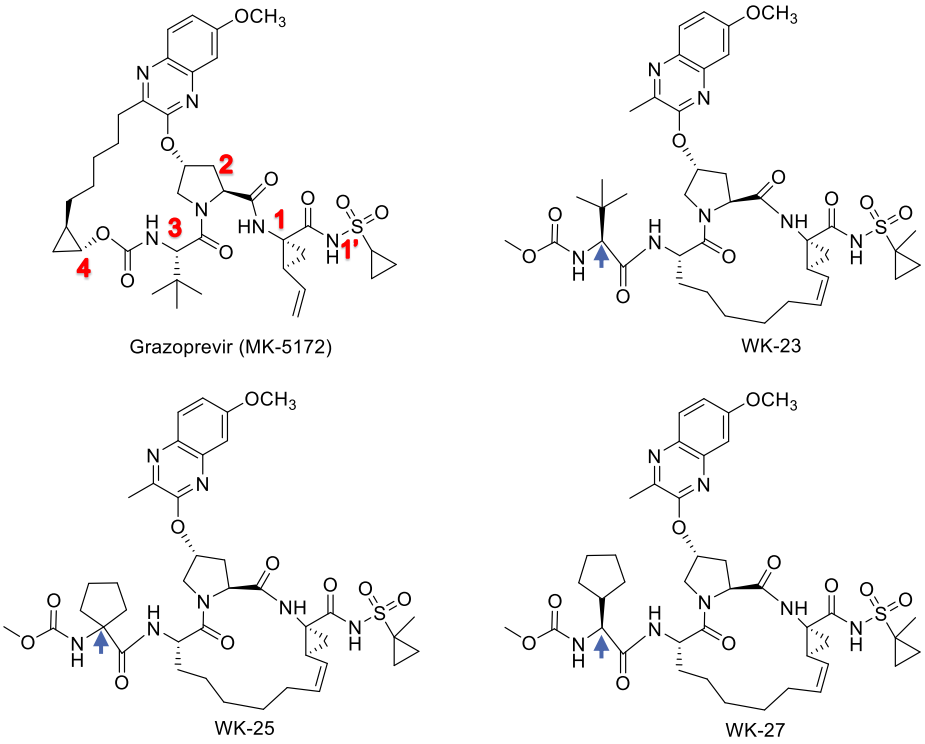

Figure **8**: PIs of focus in this study. Peptide numbering labelled in red on MK-5172. P4 group indicated with a blue arrow on novel PIs.

The purpose of this study was to synthesize three analogues of the P1-P3 macrocyclic version of MK-5172 with differing functional groups at the P4 location with an extended capping group at P5(figure 8). After synthesizing these molecules, they were tested using real-time fluorescence based enzyme inhibition assays to analyze the K_i values for each compound against wild-type GT1 protease and the D168A mutant. The goal of these experiments was to try and identify possible functional changes to these areas that can increase PI efficacy against drug-resistant variants while still maintaining nanomolar K_i values for the wild-type GT1 protease.

3 METHODOLOGY

3.1 PROTEASE INHIBITOR SYNTHESIS

3.1.1 WK-3

1-(tert-butyl) 2-methyl (2S,4S)-4-(((4-bromophenyl)sulfonyl)oxy)pyrrolidine-1,2-dicarboxylate

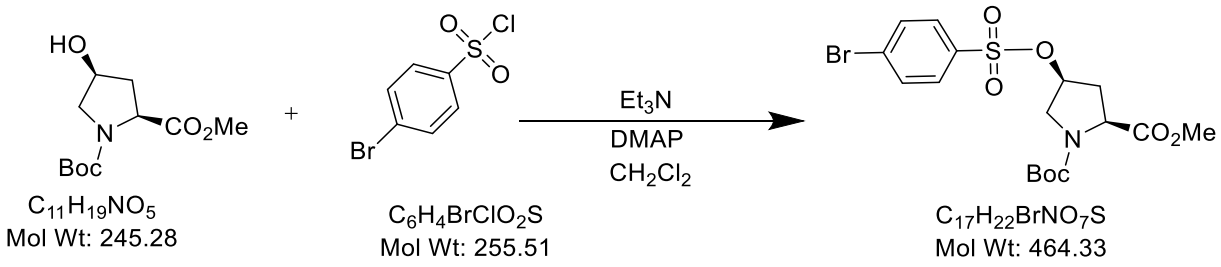

Figure **9**-WK-3 Reaction scheme

N-Boc-cis-4-hydroxy-L-proline methyl ester (10.15 g, 41.4 mmol) was mixed into anhydrous CH_2Cl_2 (75 mL) under argon atmosphere at 0 ^oC. The mixture was treated with Et3N (28.7 mL, 205.8 mmol) slowly over 15 minutes. Solid 4-bromobenzylsulfonylchloride (21.15 g, 82.8 mmol) was added followed by DMAP (0.3 g). The mixture was stirred for another 30 minutes at 0 ^oC and then stored at 5 ^oC for 24 hours. The mixture was slowly warmed to room temperature, diluted with CH_2Cl_2 (200 mL) and washed with saturated aqueous $NaHCO_3$ solution and 10% citric acid solution. The organic portion was dried with Na_2SO_4, filtered and evaporated under reduced pressure. The residue was purified by flash column chromatography using 0-10% EtOAc/CH_2Cl_2 mixture, yielding a yellow gummy solid WK-3 (16.92 g, 88%).

3.1.2 WK-9

1-(tert-butyl) 2-methyl (2S,4R)-4-((7-methoxy-3-methylquinoxalin-2-yl)oxy)pyrrolidine-1,2-dicarboxylate

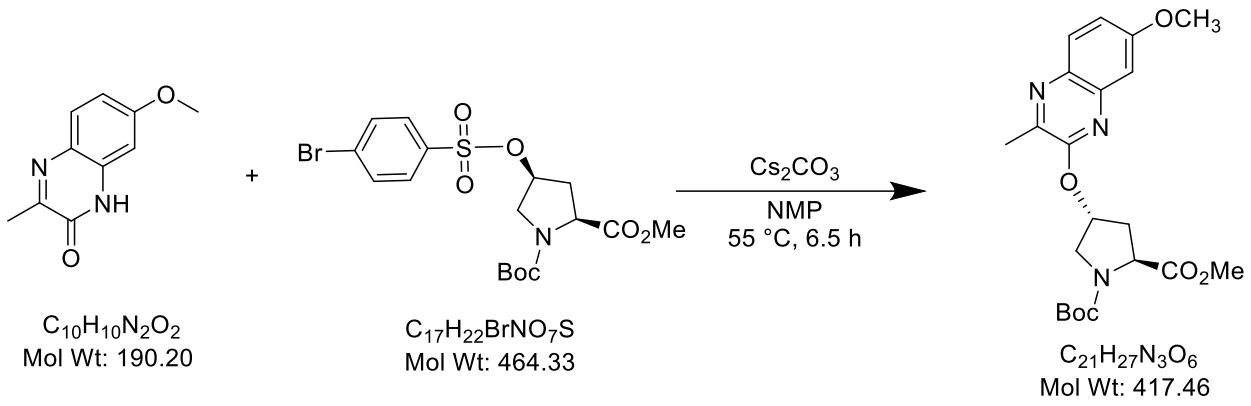

Figure **10**-WK-9 reaction scheme

3-methyl-7methoxyquinoxalin-2-one (3.8g, 20mmol) was dissolved in NMP under argon atmosphere. Cs_2CO_3 (9.8g, 30mmol) was added and the mixture was stirred for 15 minutes at room temperature. WK-3 (8.6g, 18 mmol) was added and the mixture was heated to 55^{o}C and kept stirring for 4 hours. WK-3 (0.6g, 1.3mmol) was again added after 4 hours, and the solution was mixed for another 2 hours. The reaction mixture was cooled to room temperature and diluted with 1N HCl (125mL) to pH=3. The mixture was diluted with EtOAc (300mL) and the organic fraction was extracted and washed with saturated aqueous $NaHCO_3$ and NaCl solutions (2x 250mL). The extraction was then dried with Na_2SO_4 and purified with flash column chromatography using a solvent system of 0-65% EtOAc/hexanes. The compound WK-9 eluted with 35-45% EtOAc/hexanes and was evaporated under reduced pressure to produce a white, foamy solid (6.36 g, 77% yield). ^{1}H NMR (500 MHz, $CDCl_3$) (mixture of rotamers, major rotamer) δ 7.80 (d, J = 9.0 Hz, 1 H), 7.17 (m, 1 H), 7.11 (d, J = 2.5 Hz, 1 H), 5.71 (t, J = 2.0 Hz,

1 H), 4.48 (t, *J* = 8.0 Hz, 1 H), 3.99–3.91 (m, 4 H), 3.87 (d, *J* = 12.5 Hz, 1H), 3.78 (s, 3 H), 2.67–2.58 (m, 1 H), 2.56 (s, 3 H), 2.43–2.37 (m, 1 H), 1.43 (s, 9 H) ppm; ^{13}C NMR (125 MHz, $CDCl_3$) δ 173.36, 160.24, 155.51, 153.81, 144.60, 141.04, 134.22, 128.95, 118.63, 105.95, 80.54, 73.59, 58.20, 55.68, 52.48, 52.20, 36.70, 28.26 (3 × C), 19.93 ppm; HRMS (ESI) *m/z*: calcd for $C_{21}H_{28}N_3O_6$ [M + H]+ 418.1978; found 418.19xx.

3.1.3 WK-11

(2S,4R)-4-((7-methoxy-3-methylquinoxalin-2-yl)oxy)-2-(methoxycarbonyl)pyrrolidin-1-ium chloride

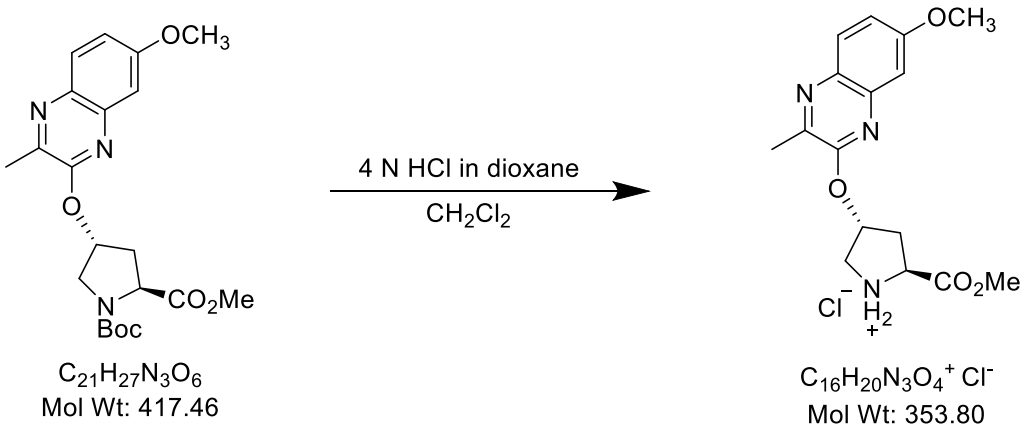

$C_{21}H_{27}N_3O_6$
Mol Wt: 417.46

$C_{16}H_{20}N_3O_4^+ Cl^-$
Mol Wt: 353.80

Figure **11**-WK-11 Reaction scheme

WK-09 (16.26g, 39 mmol) was added to CH_2Cl_2 (40mL) and stirred at room temperature until completely dissolved. 4N HCl in dioxane (40mL) was added to the reaction mixture and placed under argon atmosphere for 3 hours. The solvent was evaporated under reduced pressure and triturated with diethyl ether (3x 20mL), yielding a yellow powder, WK-11 (14.17g, 100%).

3.1.4 WK-13

Methyl (2S,4R)-1-((S)-2-((tert-butoxycarbonyl)amino)non-8-enoyl)-4-((7-methoxy-3-methylquinoxalin-2-yl)oxy)pyrrolidine-2-carboxylate

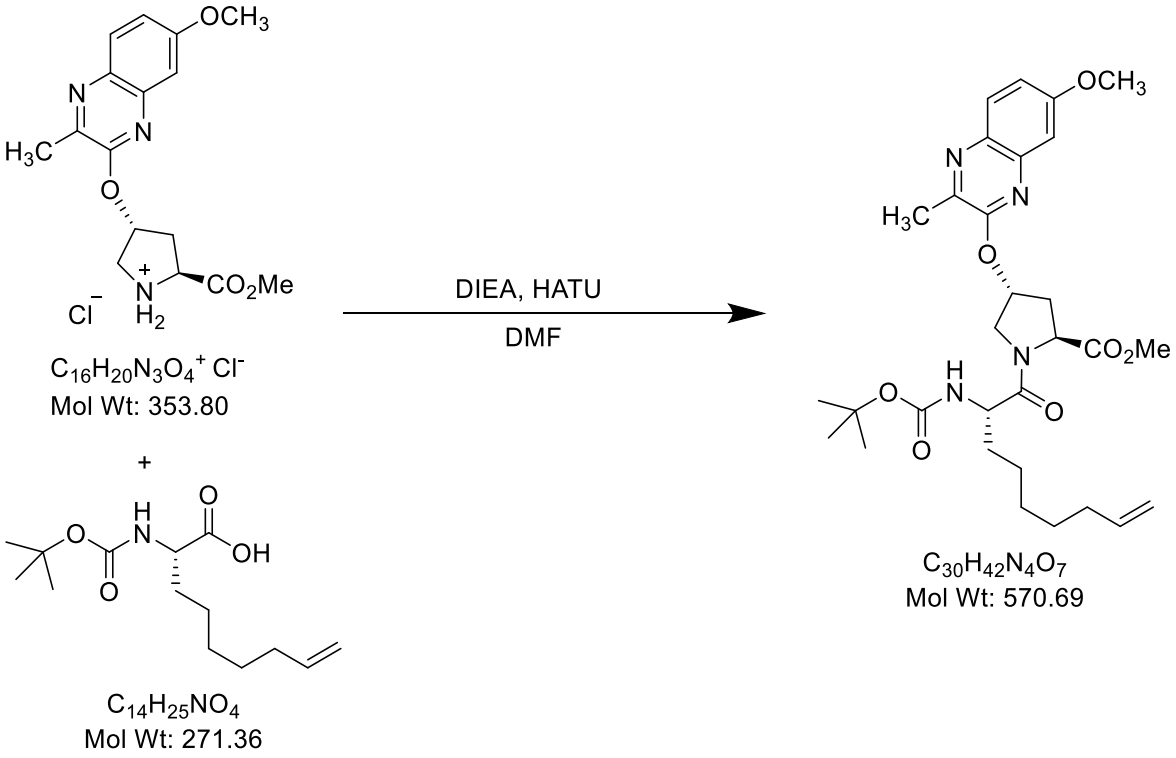

Figure **12**-WK-13 Reaction scheme

WK-11 (14.17g, 40 mmol) was added to (s)-2((tertbutoxycarbonyl)amino)non-8-enoic acid (11.0g, 40.5 mmol) in anhydrous DMF (200mL). After stirring the reaction mixture for 15 minutes at 0^{o}C, DIEA (26.8 mL, 162.0 mmol) was added slowly over 7 minutes. HATU (23.2 g, 61 mmol) was then added and the reaction was stirred at RT for 4 hours under argon atmosphere. The mixture was diluted with EtOAc (300mL) and the organic extraction was washed with 0.5N HCl, saturated aqueous $NaHCO_3$, and saturated NaCl solutions (200 mL each). The organic portion was dried with Na_2SO_4 and evaporated under reduced pressure. The residue was purified via flash column chromatography with 0-70% EtOAc/hexanes as the solvent system. The compound eluted at 40% EtOAc/hexanes to provide WK-13, a white foamy solid (14.12g, 61%).

^{1}H NMR (500 MHz, $CDCl_3$) δ 7.81 (d, J = 9.0 Hz, 1 H), 7.18 (dd, J = 9.0, 2.5 Hz, 1 H), 7.12 (d, J = 2.5 Hz, 1 H), 5.84–5.75 (m, 2 H), 5.21 (d, J = 8.5 Hz, 1 H), 4.99 (dd, J = 17.0, 1.6 Hz, 1 H), 4.93 (dd, J = 8.8, 1.2 Hz, 1 H), 4.75 (t, J = 8.0 Hz, 1 H), 4.38 (q, J = 7.5 Hz, 1 H), 4.18 (d, J = 11.5 Hz, 1 H), 4.06 (dd, J = 12.0, 4.5 Hz, 1 H), 3.94 (s, 3 H), 3.77 (s, 3 H), 2.69–2.64 (m, 1 H), 2.54 (s, 3 H), 2.41–2.35 (m, 1 H), 2.04 (app q, J = 7.0 Hz, 2 H), 1.80–1.75 (m, 1 H), 1.63–1.55 (m, 1 H), 1.46–1.25 (m, 16 H) ppm; ^{13}C NMR (125 MHz, $CDCl_3$) δ 172.13, 171.78, 160.27, 155.40, 155.27, 144.62, 140.89, 138.96, 134.39, 129.03, 118.73, 114.35, 105.99, 79.61, 74.30, 57.97, 55.66, 52.67, 52.43, 51.83, 37.03, 34.94, 33.65, 32.66, 28.91, 28.74, 28.25, 24.68, 19.87 ppm; HRMS (ESI) *m/z*: calcd for $C_{30}H_{43}N_4O_7$ $[M + H]^+$ 571.3132; found 571.31xx.

3.1.5 WK-15

(2S,4R)-1-((S)-2-((tert-butoxycarbonyl)amino)non-8-enoyl)-4-((7-methoxy-3-methylquinoxalin-2-yl)oxy)pyrrolidine-2-carboxylic acid

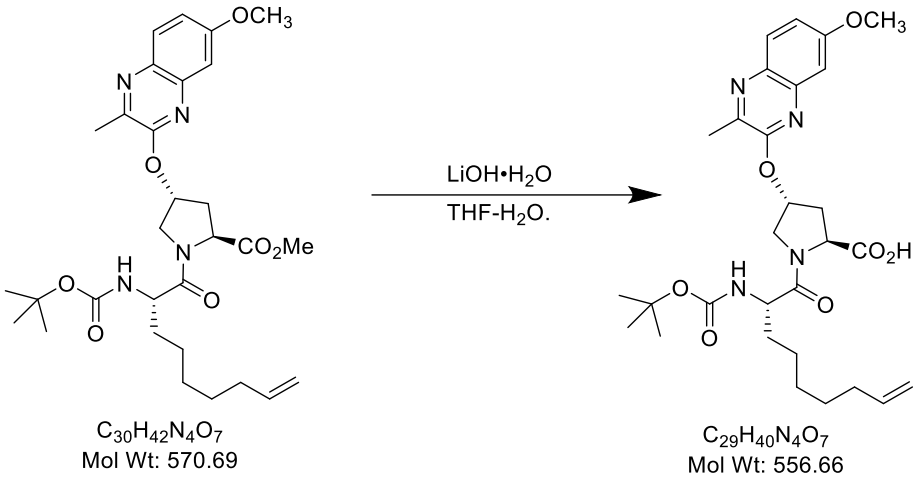

Figure **13**: WK-15 Reaction Scheme

A solution of WK-13(12.3 g, 21.55mmol) in THF-H_2O (150mL) was treated with LiOH-H_2O (2.94 g, 70mmol). The reaction was stirred at room temperature for 24 hours and then

cooled to 5°C and acidified with 0.5N HCl (200ml) to pH<2. The mixture was diluted with EtOAc(1000mL) and washed with saturated aqueous NaCl (250mL). The organic fractions was dried with Na_2SO_4, filtered and evaporated under reduced pressure. The residue was dissolved in $CHCl_3$ (50mL) and evaporated again under reduced pressure. The residue was subsequently dried under high vacuum overnight and yielded WK-15 (11.96 g, 100%).

3.1.6 WK-17

Tert-butyl ((S)-1-((2S,4R)-4-((7-methoxy-3-methylquinoxalin-2-yl)oxy)-2-(((1R,2S)-1-(((1-methylcyclopropyl)sulfonyl)carbamoyl)-2-vinylcyclopropyl)carbamoyl)pyrrolidin-1-yl)-1-oxonon-8-en-2-yl)carbamate

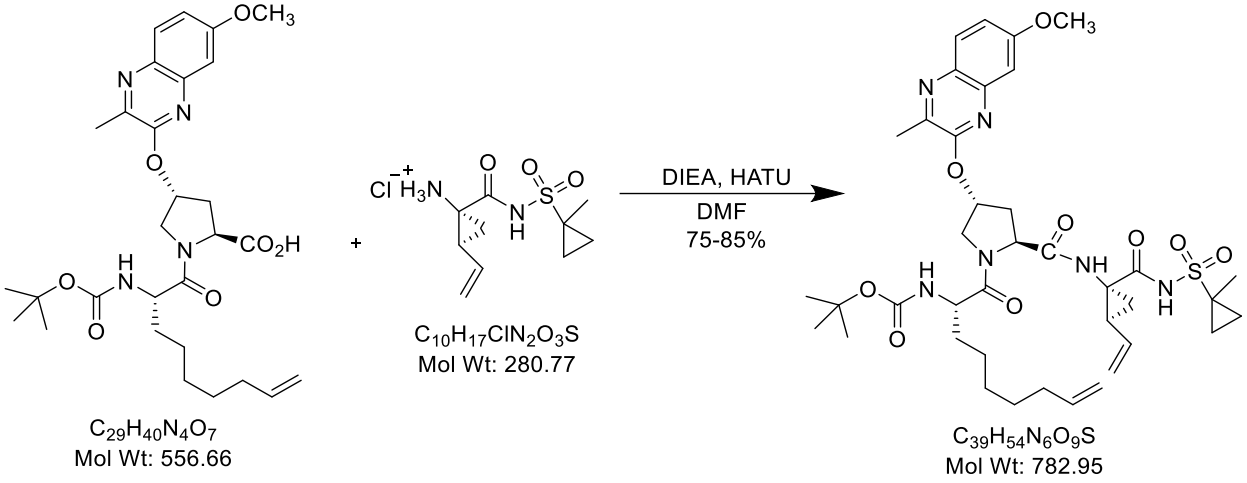

Figure **14**: WK-17 reaction scheme

WK-15 (7.0g, 12.57mmol) and (1R,2S)-1-(((1-methylcyclopropyl)sulfonyl)carbamoyl)-2-vinylcyclopropan-1-aminium chloride (4g, 14.24mmol) were added to DMF (115mL) and stirred at room temperature until a solution was made. DIEA (8.3mL, 50.3mmol) was added immediately followed by HATU (7.5g, 19.7mmol) and the reaction was stirred for 3 hours. The mixture was diluted with EtOAc (700ml) and washed with 0.5N HCl (400ml), 50% $NaHCO_3$

solution (300ml) and saturated NaCl solution (300ml). The organic portion was dried over Na_2SO_4 and evaporated. The residue was purified via flash column chromatography using a solvent system of 20-90% EtOAc/hexanes. 20g silica gel was added to the residue and 2 aliquots of the solid were purified using 80g gold silica columns, the compound eluted with 50-70% EtOAc/hexanes and the column ran for a total of 32 minutes. The residue was evaporated under reduced pressure and yielded WK-17 (8.30g, 84.3%). ^{1}H NMR (400 MHz, $CDCl_3$) δ 10.02 (s, 1 H), 7.81 (d, *J* = 8.8 Hz, 1 H), 7.18 (dd, *J* = 8.8, 2.8 Hz, 1 H), 7.13 (d, *J* = 2.8 Hz, 1 H), 7.11 (s, 1 H), 5.88 (br s, 1 H), 5.82–5.72 (m, 2 H), 5.42 (d, *J* = 9.2 Hz, 1 H), 5.26 (d, *J* = 17.2 Hz, 1 H), 5.14 (d, *J* = 11.6 Hz, 1 H), 5.0–4.90 (m, 2 H), 4.50 (t, *J* = 8.4 Hz, 1 H), 4.39–4.33 (m, 1 H), 4.18 (d, *J* = 11.6 Hz, 1 H), 4.02 (dd, *J* = 11.6, 4.0 Hz, 1 H), 3.93 (s, 3 H), 2.58–2.50 (m, 2 H), 2.53 (s, 3 H), 2.10 (q, *J* = 8.4 Hz, 1 H), 2.04–1.98 (m, 2 H), 1.73–1.58 (m, 2 H), 1.49 (s, 3 H), 1.44–1.24 (m, 8 H), 1.35 (s, 9 H), 0.92–0.86 (m, 1 H), 0.84–0.78 (m, 1 H); ^{13}C NMR (100 MHz, $CDCl_3$) δ 173.65, 172.52, 167.55, 160.31, 155.70, 155.16, 144.41, 140.87, 138.83, 134.33, 132.61, 128.96, 118.87, 118.54, 114.41, 105.96, 79.93, 74.59, 60.30, 55.67, 53.15, 52.37, 41.73, 35.56, 35.16, 34.25, 33.62, 32.24, 28.71, 28.67, 28.26 (3C), 25.31, 23.42, 19.84, 18.37, 14.27, 13.26 ppm; HRMS (ESI) *m/z*: calcd for $C_{39}H_{55}N_6O_9S$ $[M + H]^+$ 783.3751; found 783.37xx.

3.1.7 WK-19

Tert-butyl ((2R,6S,13aS,14aR,16aS,Z)-2-((7-methoxy-3-methylquinoxalin-2-yl)oxy)-14a-(((1-methylcyclopropyl)sulfonyl)carbamoyl)-5,16-dioxo-1,2,3,5,6,7,8,9,10,11,13a,14,14a,15,16,16a-hexadecahydrocyclopropa[e]pyrrolo[1,2-a][1,4]diazacyclopentadecin-6-yl)carbamate

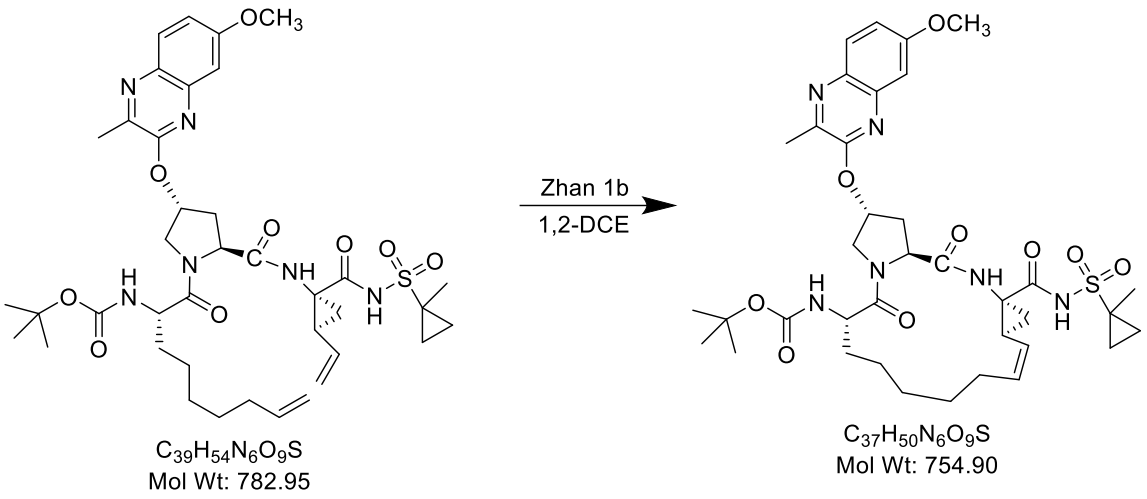

Figure **15:** WK-19 Reaction Scheme

Bis-Olefin WK-17 (8.2g, 10.4mmol) was dissolved in 1,2-dicholoroethane (1600ml) and degassed and placed under argon atmosphere. The solution was heated to 50°C and Zhan 1b catalyst (0.50g, 0.67mmol) was added in two portions overs 10 minutes. The reaction was heated to 70°C and stirred under argon atmosphere for 6 hours. The mixture was cooled to room temperature and solvent were evaporated under reduced pressure. The residue was purified via flash column chromatography by running two 80g gold silica columns at 25-90% EtOAc/hexanes for 32 minutes. The compound WK-19 (5.18g, 66%) eluted at 50-70% EtOAc/hexanes. ^{1}H NMR (400 MHz, $CDCl_3$) δ 10.16 (s, 1H), 7.82 (d, J = 9.2 Hz, 1H), 7.19–7.16 (m, 2H), 6.92 (s, 1H), 5.88 (br s, 1H), 5.69 (q, J = 9.2 Hz, 1H), 5.12 (d, J = 7.6 Hz, 1H), 4.99 (t, J = 8.8 Hz, 1H), 4.61 (t, J = 8.0 Hz, 1H), 4.51 (d, J = 11.2 Hz, 1H), 4.25 (m, 1H), 4.03 (dd, J = 11.2, 4.0 Hz, 1H), 3.95 (s, 3H), 2.65 (m, 1H), 2.58 (m, 3H), 2.53 (s, 3H), 1.92–1.73 (m, 3H), 1.60–1.30 (m, 6H), 1.48 (s, 3H), 1.27 (s, 9H), 0.85–0.78 (m, 2H) ppm; ^{13}C NMR (100 MHz, $CDCl_3$) δ 177.16, 173.33, 166.94, 160.33, 155.32, 155.04, 144.46, 141.03, 136.25, 128.66, 124.89, 118.93, 105.98, 79.85, 74.88, 59.46, 55.72, 53.08, 51.97, 44.73, 36.43, 34.61, 32.72,

29.65, 28.15 (3C), 27.06, 26.07, 22.21, 20.96, 19.71, 18.17, 14.51, 12.51 ppm; HRMS (ESI) *m/z*: calcd for $C_{37}H_{51}N_6O_9S$ $[M + H]^+$ 755.3433; found 755.3404.

3.1.8 WK-21

(2R,6S,13aS,14aR,16aS,Z)-2-((7-methoxy-3-methylquinoxalin-2-yl)oxy)-14a-(((1-methylcyclopropyl)sulfonyl)carbamoyl)-5,16-dioxo-1,2,3,5,6,7,8,9,10,11,13a,14,14a,15,16,16a-hexadecahydrocyclopropa[e]pyrrolo[1,2a][1,4]diazacyclopentadecin-6-aminium chloride

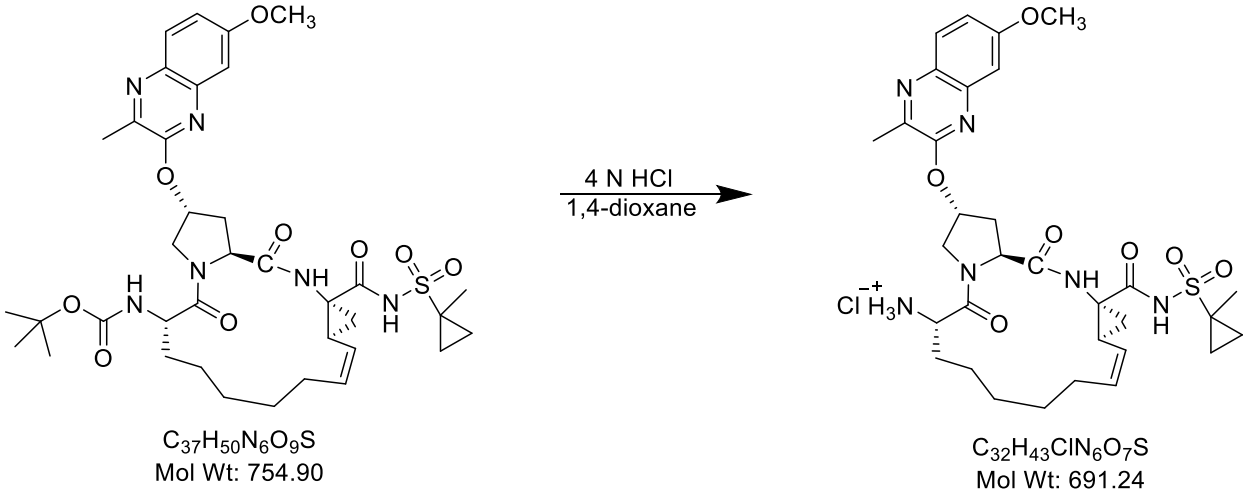

Figure **16:** WK-21 Reaction Scheme

WK-19 (1.06g, 1.40mmol) was treated with 4N HCl in 1,4-dioxane (30ml) at room temperature under argon atmosphere for 3 hours. The solvent was evaporated under reduced pressure and triturated with diethyl ether (2x 20mL). The solvent was evaporated under reduced pressure to yield gray solid WK-21 (0.8g, 83%).

3.1.9 WK-23

Methyl ((R)-1-(((2R,6S,13aS,14aR,16aS,Z)-2-((7-methoxy-3-methylquinoxalin-2-yl)oxy)-14a-(((1-methylcyclopropyl)sulfonyl)carbamoyl)-5,16-dioxo-1,2,3,5,6,7,8,9,10,11,13a,14,14a,15,16,16a-hexadecahydrocyclopropa[e]pyrrolo[1,2-a][1,4]diazacyclopentadecin-6-yl)amino)-3,3-dimethyl-1-oxobutan-2-yl)carbamate

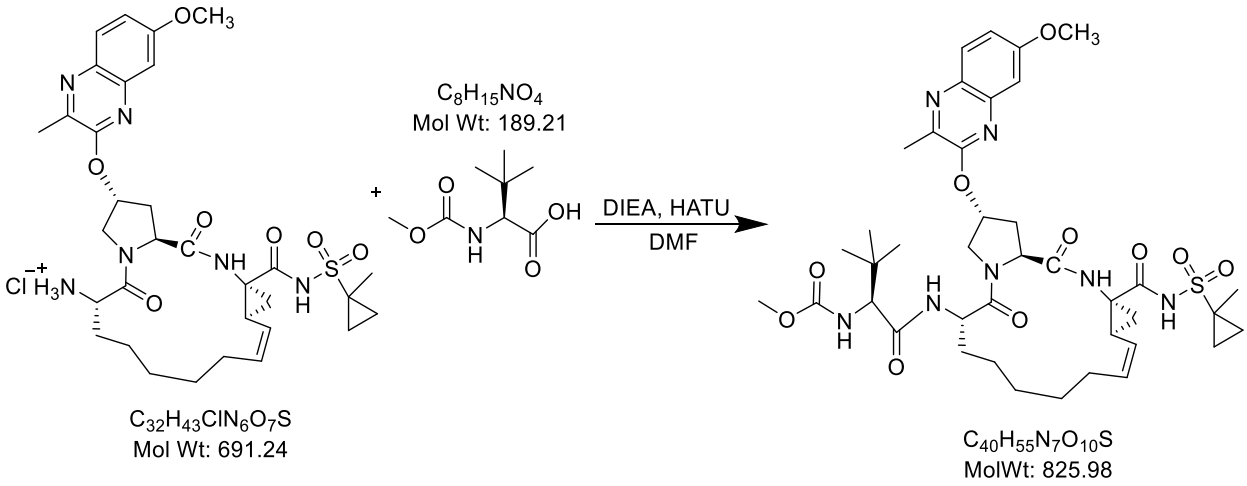

Figure **17:** WK-23 Reaction Scheme

WK-21 (0.250g, 0.36mmol) was mixed with DMF (8mL) and methoxycarbonyl-L-tert-Leucine (0.093g, 0.48mmol). DIEA (0.45ml, 2.35mmol) was added over 3 minutes followed by HATU (0.3g, 0.75mmol) and the reaction mixture was stirred at room temperature under argon atmosphere. After 4 hours, the solution was diluted with EtOAc (200ml) and washed with 0.5N HCl (125mL), 50% $NaHCO_3$ solution (125ml) and saturated NaCl solution (125ml). The organic fraction was dried with Na_2SO_4 and evaporated under reduced pressure.

1g of silica was added to the residue and it was purified via flash column chromatography. A 24g gold silica column was used and ran with a solvent system of 30-100% EtOAc/hexanes for 21 minutes, the compound WK-23 (0.250g, 84%) eluted at 60% EtOAc/hexanes and was

evaporated under reduced pressure. ^{13}C NMR (125 MHz, $CDCl_3$) δ 176.64, 172.83, 169.25, 166.82, 160.45, 157.58, 155.03, 143.64, 141.01, 136.80, 134.33, 128.88, 124.79, 119.12, 106.00, 78.98, 62.16, 59.14, 55.76, 54.01, 53.125, 50.24, 43.98, 36.53, 35.28, 34.99, 34.84, 34.26, 28.63, 27.45, 27.38, 26.62, 26.40, 22.78, 19.81, 19.69, 18.20, 14.46, 12.62

3.1.10 WK-25

Methyl (1-(((2R,6S,13aS,14aR,16aS,Z)-2-((7-methoxy-3-methylquinoxalin-2-yl)oxy)-14a-(((1-methylcyclopropyl)sulfonyl)carbamoyl)-5,16-dioxo-1,2,3,5,6,7,8,9,10,11,13a,14,14a,15,16,16a-hexadecahydrocyclopropa[e]pyrrolo[1,2-a][1,4]diazacyclopentadecin-6-yl)carbamoyl)cyclopentyl)carbamate

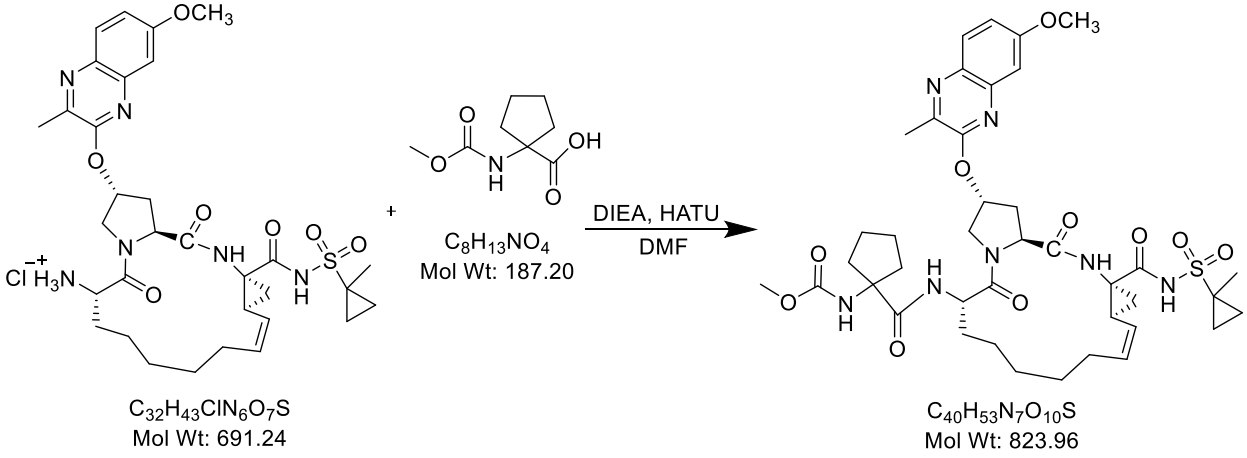

Figure **18**: WK-25 Reaction Scheme

WK-21 (0.250g, 0.36mmol) was mixed with DMF (8mL) and methoxycarbonyl-cycloleucine (0.089g, 0.48mmol). DIEA (0.45ml, 2.35mmol) was added over 3 minutes followed by HATU (0.3g, 0.75mmol) and the reaction mixture was stirred at room temperature under argon atmosphere. After 4 hours, the solution was diluted with EtOAc (200ml) and washed with 0.5N HCl (125mL), 50% $NaHCO_3$ solution (125ml) and saturated NaCl solution (125ml). The organic fraction was dried with Na_2SO_4 and evaporated under reduced pressure.

1g of silica was added to the residue and it was purified via flash column chromatography. A 24g gold silica column was used and ran with a solvent system of 60-100% EtOAc/hexanes for 18 minutes and yielded the compound WK-25 (0.200g, 67%) which was dried under reduced pressure. ^{13}C NMR (125 MHz, $CDCl_3$) δ 176.82, 173.83, 172.89, 167.22, 160.31, 156.13, 155.27, 144.29, 141.00, 136.32, 134.35, 128.29, 125.13, 118.89, 106.06, 74.63, 66.92, 59.21, 55.75, 52.84, 52.21, 51.53, 44.37, 38.61, 37.80, 36.49, 36.06, 34.51, 32.12, 29.69, 27.71, 27.11, 25.93, 24.11, 22.55, 19.81, 18.13, 14.64, 12.51.

3.1.11 WK-27

Methyl ((R)-1-cyclopentyl-2-(((2R,6S,13aS,14aR,16aS,Z)-2-((7-methoxy-3-methylquinoxalin-2-yl)oxy)-14a-(((1-methylcyclopropyl)sulfonyl)carbamoyl)-5,16-dioxo-1,2,3,5,6,7,8,9,10,11,13a,14,14a,15,16,16a-hexadecahydrocyclopropa[e]pyrrolo[1,2-a][1,4]diazacyclopentadecin-6-yl)amino)-2-oxoethyl)carbamate

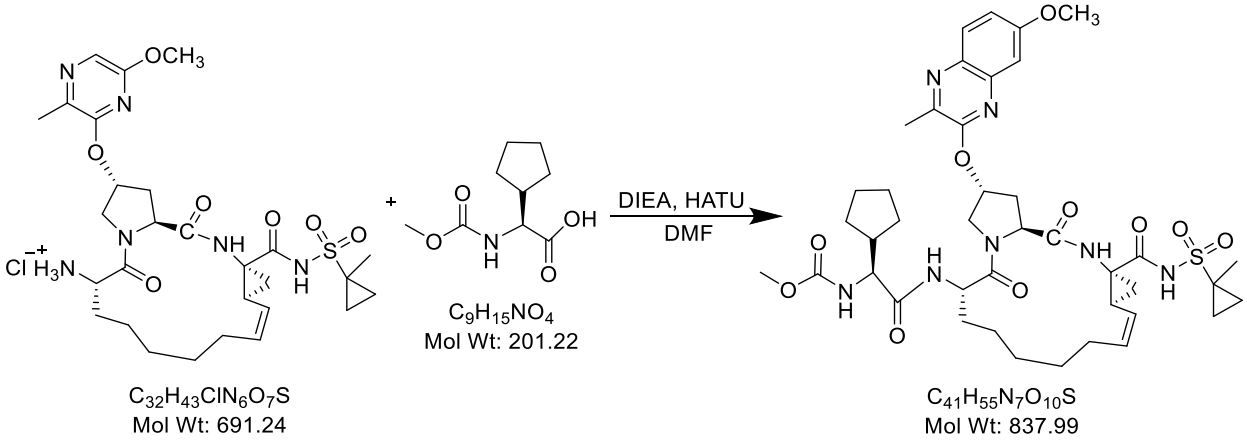

Figure **19:** WK-27 Reaction Scheme

WK-21 (0.250g, 0.36mmol) was mixed with DMF (8mL) and methoxycarbonyl-L-cylcopentlylglycine (0.096g, 0.48mmol) at room temperature. DIEA (0.45ml, 2.35mmol) was added over 3 minutes followed by HATU (0.3g, 0.75mmol) and the reaction mixture was stirred under argon atmosphere for 4 hours. After 4 hours, the solution was diluted with EtOAc (200ml)

and washed with 0.5N HCl (125mL), 50% $NaHCO_3$ solution (125ml) and saturated NaCl solution (125ml). The organic fraction was dried with Na_2SO_4 and evaporated under reduced pressure.

1g of silica was added to the residue and it was purified via flash column chromatography. A 24g gold silica column was used and ran with a solvent system of 50-100% EtOAc/hexanes for 16 minutes and yielded the compound WK-27 (0.250g, 83%) which was dried under reduced pressure. ^{13}C NMR (125 MHz, $CDCl_3$) δ 177.01, 173.32, 170.49, 166.95, 160.46, 157.82, 155.15, 143.75, 141.02, 136.74, 134.36, 128.91, 124.74, 119.14, 106.02, 74.92, 59.26, 56.15, 55.78, 53.91, 53.14, 50.15, 44.16, 43.45, 38.61, 36.50, 35.34, 34.56, 29.28, 28.63, 27.53, 27.39, 26.69, 25.46, 25.26, 22.29, 19.54, 18.21, 14.56, 12.59.

3.2 EXPRESSION AND PURIFICATION OF HCV PROTEASES

A culture of BL-21 (DE3) *E. coli* cells was transformed with a plasmid encoding for the NS3/4a HCV protease. The culture was plated overnight and transferred to a flask with 45µl of 10mg/ml kanamycin solution and 15 mL LB broth. The flask was incubated at 37ºC for 6 hours. The culture was then diluted to 1L with LB broth and 600 µl of 10mg/mL kanamycin was added and continued to incubate at 37ºC overnight.

Six 150 mL aliquots of the culture were subsequently separated into culture flasks and diluted to 1L of LB broth. The cultures were incubated at 37ºC for 3-4 hours until OD600 was 0.6, when 1ml of 1M IPTG was added to each flask. The cultures were incubated at 18ºC overnight and subsequently centrifuged at 5000rpm for 15 minutes.

The cells were resuspended with 50mM sodium phosphate resuspension buffer (pH=7.5) and mixed with DNAse and 10mL of 2mM $MgCl_2$ solution. The pellet was then homogenized using a cell disrupter and centrifuged for 25 minutes at 5000rpm. The supernatant was flash frozen and stored at -80^{o}C until purified.

The supernatant (crude extract) was purified using 7mL of nickel resin. The resin was equilibrated with resuspension buffer and the crude extract was subsequently added. The resin was allowed to equilibrate with the crude extract for 1.5 hours on a nutator at 4^{o}C. The buffer was allowed to flow through and allow the nickel resin to adsorb the His-tagged protein. The protein was eluted with 500mM imidazole solution and stored at -80^{o}C.

3.3 ENZYME INHIBITION ASSAYS

The purpose of the inhibition assays was to quantify the inhibition for each synthesized compound on HCV protease activity for GT-1a and D168A constructs. The substrate used was a 5-FAM/QXL 520 peptide substrate that flouresces at 520nm when cleaved. To determine the K_i of the inhibitors MK-5172 and WK-27 against wild-type protease, a 2:3 serial dilution of 50nm protease inhibitor (PI) solution was used. For inhibitors WK-23 and WK-25, a 1:2 dilution of 200nM PI in the first well was used instead. For the D168A mutant, a 1:2 serial dilution of 2.4μM PI concnentration was used.

The concentration of protein was kept constant at 2nM and the buffer in the well consisted of 50mM Tris pH 7.5, 5% glycerol, 10mM Dithiothreitol (DTT), 0.6mM Lauryl dimethylamine N-oxide (LDAO), and 4% DMSO. All components aside from the substrate were added to a Corning 96-well plate and incubated for 1 hour at room temperature. Each well in the plate was

then rapidly injected with 5µl of 200nM substrate solution and the plate was read with a Perkin-Elmer EnVision plate reader with an excitation filter at 485 nm and emission filter at 530nm).

4 RESULTS

The goal of the project was to synthesize HCV NS3/4a protease inhibitors and analyze their inhibition potency using the kinetic assays detailed above. The core molecule WK-19 was intended to be a P1-P3 macrocyclic analogue of MK-5172 with a modified P1' residue with a methylcyclopropyl sulfonamide and methylquinoxaline at the P2 location. 200 mg aliquots of WK-21 were used to synthesize 3 different final PIs WK-23, WK-25, and WK-27.

The PIs were then analyzed using kinetic assays and the K_i values were compared to MK-5172 K_i that was also determined.

4.1 SYNTHESIS OF PIS

The molecule WK-19 was synthesized by coupling the P2-P3 fragment (WK-15) with the amine salt of the P1-P1' fragment (figure 13) and then undergoing a ring closing metathesis reaction to close the P1-P3 macrocycle (figure 14). This yielded a total of 5.18 g of the core molecule WK-19. Before synthesizing the final compounds with modified P4 groups, the t-butyl ester at the P3 position was hydrolyzed to yield the amine salt WK-21, which could be used in peptide coupling reactions. A 1.06g (1.40mmol) aliquot of WK-19 was hydrolyzed with 4N HCl in 1,4-dioxane and the process yielded 0.8g (1.16mmol) of WK-21.

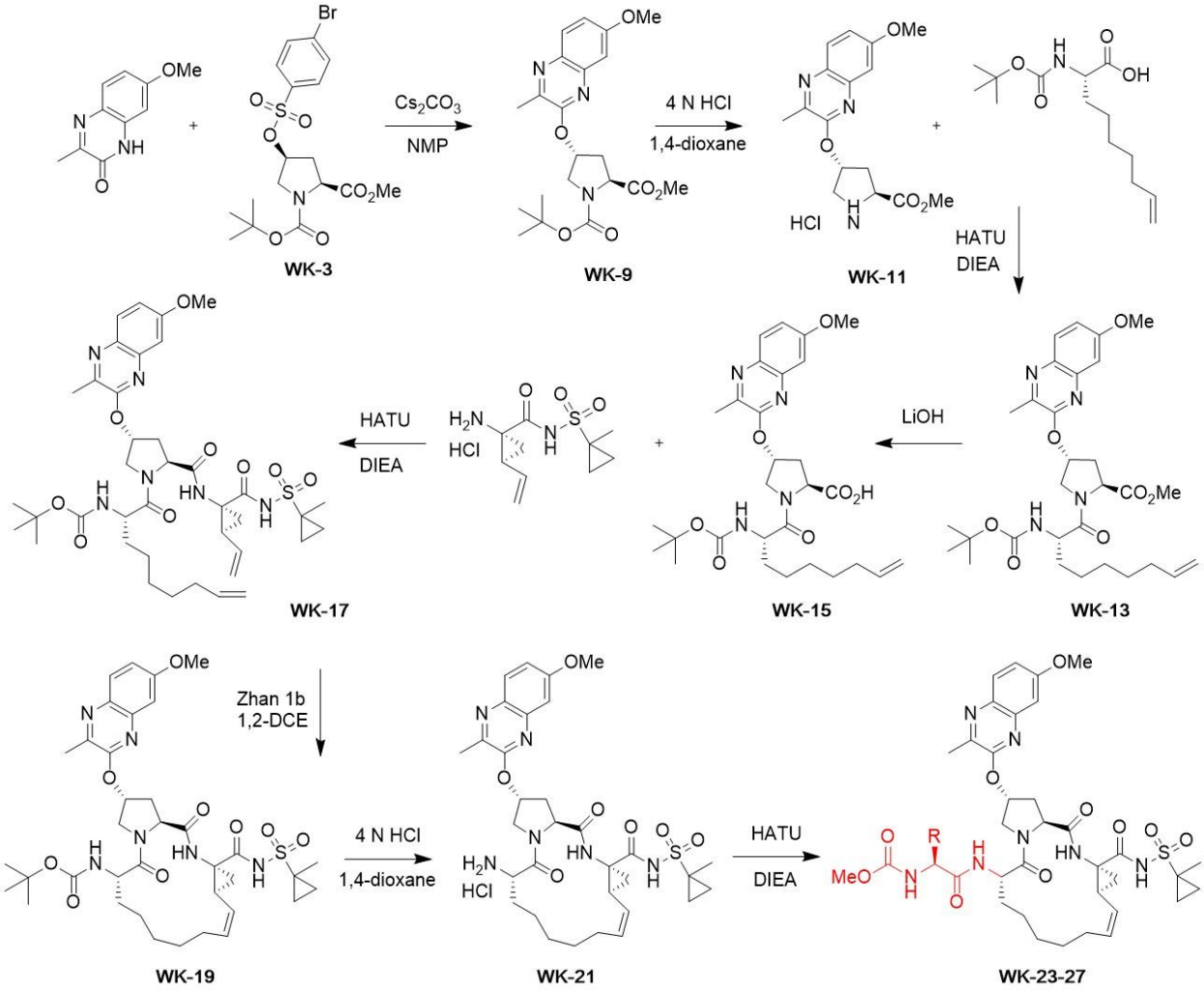

Figure 20: Overall scheme of PI synthesis.

To make the PIs, 0.250 g (0.36 mmol) of WK-21 was used in each peptide coupling reaction. 0.48 mmol of the corresponding P4 capping group (figure 19) was added along with diisopropylethylamine (DIEA) and HATU. The products of each reaction yielded ~0.3mmol of each protease inhibitor which were subsequently used for kinetic analysis.

4.2 Enzyme Inhibition Assays

The compounds WK-23, WK-25, WK-27, and MK-5172 were analyzed for their K_i values against the wild-type GT-1a HCV NS3/4a protease. A 2:3 serial dilution of inhibitor was used with the largest well concentration being 50nM for MK-5172 and WK-27 against GT-1a protease. For the other inhibitors, a 1:2 dilution of inhibitor with the largest concentration being 200nM was used. For the D168A assay, a 1:2 dilution of inhibitor was used for all compounds and the largest starting concentration was 2.4μM. The initial velocities of each assay well were determine via linear regression analysis and were plotted against inhibitor concentration. Using the morrison equation for tight-binding inhibitors, the Ki for each compound was determined using the Vi vs [I] graph.

The K_i for Wk-27 was 4.0 +/- 0.6 nM and was the closest value to the consensus K_i of MK-5172 of 0.20 +/- 0.03 nM (table 1) against Gt-1a protease. The other two compounds (WK-23 and WK-25 were significantly less potent than MK-5172 at 28+/- 11 nM and 55+/- 9 nM.

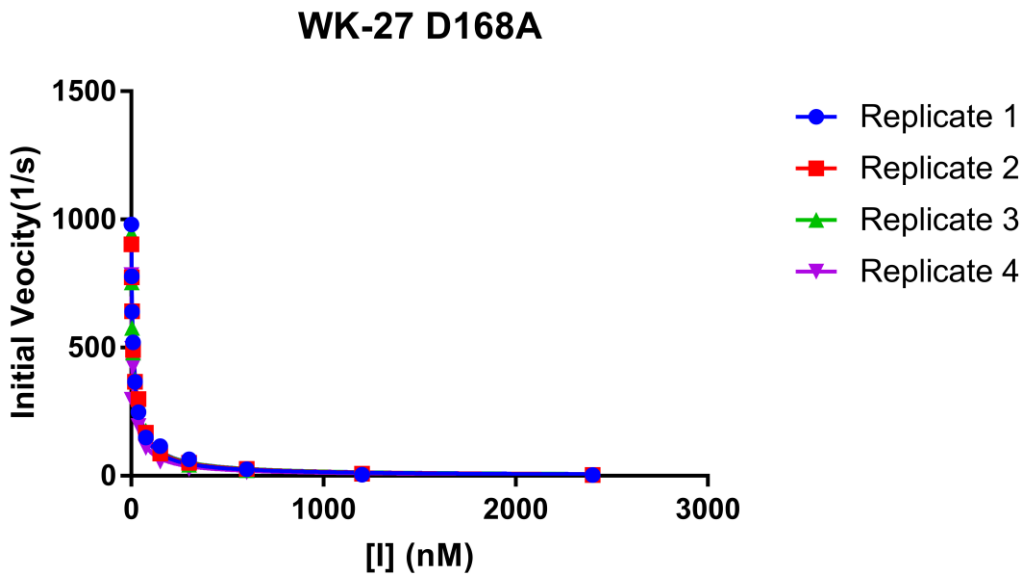

Figure **21**-Sample Vi vs [I] graph that is used to calculate the K_i of a tight binding inhibitor.

For the D168A variant, WK-27 exhibit the largest barrier to resistance with a change of only one order of magnitude at 16.17 nM +/- 2.86. WK-25 was particularly less potent with a Ki of 171.1 nM +/- 13.47. Once again, none of the WK inhibitors were as potent as MK-5172.

Table **1**: Inhibition data derived from Kinetic assays, graph of K_i values shown below.

Ki (nM)				
Structure	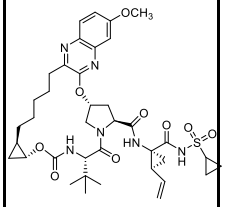	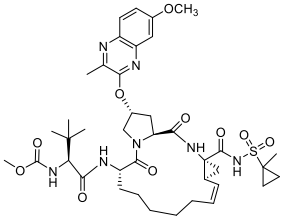	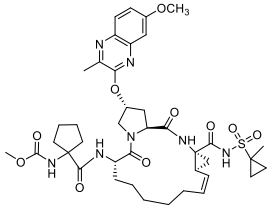	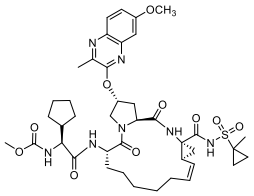
Inhibitor	MK-5172	WK-23	WK-25	WK-27
GT-1a	0.20 +/- 0.03	22.45 +/-2.39	35.68 +/- 4.61	4.00 +/- 0.60
D168A	11.08 +/- 1.01	55.09 +/- 4.83	174.1 +/- 13.47	16.17 +/- 2.86

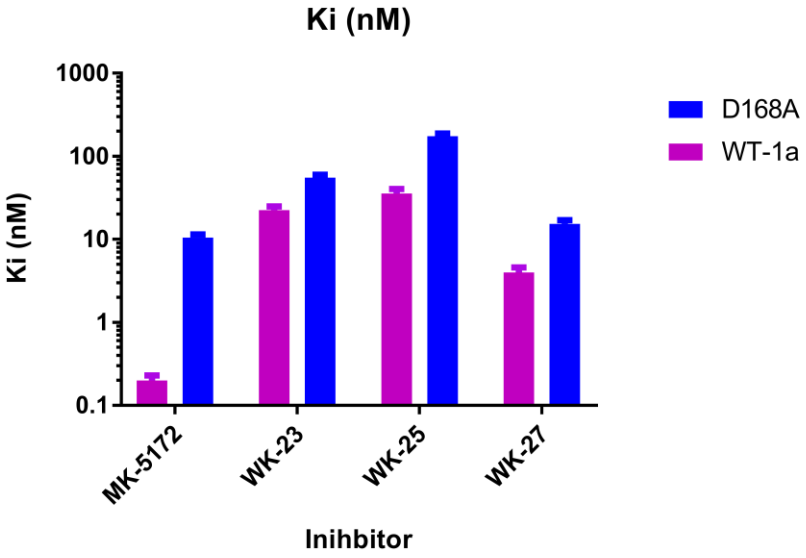

5 DISCUSSION

The NS3/4a serine protease of HCV is a key therapeutic target because of its integral role in viral maturation and proliferation. Earlier NS3/4a protease inhibitors showed promise against GT-1 wild-type proteases but were rendered useless in the event of drug-resistant mutations. Due to the error-prone RNA-dependent RNA polymerase, mutant quasispecies can arise within a patient that can become the predominant species when the selective pressure of a drug is applied. To combat this, a series of modified PIs have been synthesized by numerous companies with varying efficacies. The gold standard of treatment among these PIs is MK-5172 (Grazoprevir) developed by Merck.

5.1 PROTEASE INHIBITOR SYNTHESIS

Using MK-5172 as a template, the first goal of this project was to synthesize analogous PIs with a macrocycle connecting the P1 and P3 residues of the inhibitor instead of P2-P4 cycle in MK-5172. The result of the synthesis yielded three compounds, WK-23, WK-25, and WK-27, all of which differ in their P4 groups (figure 8). Compounds were purified using flash column chromatography with different solvent systems as previously outlined. While most compounds were not difficult to purify, WK-13 required several column runs to extract nearly all of the pure product left in the reaction mixture. After purification, the eluted fractions were analyzed via TLC to identify the pure fractions to pool and collect for subsequent synthesis steps. The final compounds were stored in DMSO at -80^{o}C.

5.2 KINETIC INHIBITION ASSAY PROCEDURE

The three compounds were subsequently analyzed for their *in vitro* inhibition properties on two variants of the HCV NS3/4a protease: GT-1a (wild type) and the D168A mutant construct. The overall procedure for the assays was straightforward, the concentration of protease and substrate remained constant and the only differing part of the assay was the inhibitor concentration. Initially, the concentrations and serial dilution of the novel PIs were kept the same as already established values for MK-5172. For GT-1a, that was a 2:3 dilution and 50nM [I] being the highest concentration in any well. While this gave good results for WK-27 and MK-5172, the values of WK-23 and 25 were more error prone and the graph of V_i and [I] was not optimal for determining the K_i. As mentioned before, the K_i was determined by fitting the V_i vs. [I] graph to the Morrison equation for tight binding inhibitors (figure 21). In order to get the most accurate K_i value from this graph, the region in the plot with the most curvature (deemed the elbow region) should contain as many points as possible, whereas the regions of the graph that are asymptotic only need 2 or 3 points.[20] For WK-23 and 25 this meant changing the concentration of inhibitor from 50nM to 200nM, and the serial dilution from 2:3 to 1:2. This resulted in a better fit for the Morrison equation and smaller error values.

5.3 INHIBITOR POTENCY AND IMPLICATIONS ON DRUG DESIGN

For the wild type protease, MK-5172 remained the most potent inhibitor (K_i=0.2 +/- 0.03 nM) with WK-27 having the closest level of inhibition with K_i = 4+/- 0.6 nM. Both WK-23 and WK-25 were much less potent with K_i values of 22.45 and 35.68 nM respectively (table 1). Slightly higher K_i values of the P1P3 macrocycles were expected for the Gt-1a protease based on

previous studies, however the nearly 100 fold increase in K_i for WK-23 and 25 was not expected.[19] Future structural studies may be able to indicate the reasoning behind the significant loss of potency for both of those variants.

For the D168A mutant, MK-5172 was again the most potent inhibitor with a K_i of 11.08 +/- 1.01 nM, however WK-27 had a flatter resistance profile by only losing potency by one order of magnitude to a K_i value of 16.17 +/- 2.86 nM. WK-25 was the main outlier with a K_i of 174.1 +/- 13.47 nM. While the minimal effect of the D168A mutation on WK-27's inhibition potency was encouraging, the K_i was still larger than that of MK-5172 which was again consistent with previous P1P3 macrocyclic inhibitors.[19] Examining inhibitor potency against other mutants like R155K and A156T proteases should help characterize the general resistance profile of each PI and give a better indication on if WK-27 in fact has a flatter resistance profile.

Cell based drug susceptibility assays using HCV replicon RNA introduced into Huh7 cells can be performed to analyze the inhibitor potency *in vivo*. In previous studies the IC50 (the drug concentration to reduce replicon replication by 50%) showed differing inhibition profiles than the kinetic assays.[19] With MK-5172 and WK-27 having very similar K_i values this may help to further differentiate their potency relative to one another.

For inhibitor design and synthesis moving forward, studies should be conducted using different P4 capping amino acid functional groups to identify any group with better overall potency. The resistance of WK-27 to the D168A mutation could also lead to experiments examining larger functional groups, considering the other two PIs (WK-23 and 25) have smaller functional groups that may not have interacted as strongly with adjacent residues from the protease. Interestingly enough, the more rigid PI (WK-25) at P4 was the least potent inhibitor (table 1). This could mean that more flexible P4 residues are better at binding to the protease and

retaining inhibition across mutants. Developing larger but more flexible residues at the P4 group could potentially increase inhibitor potency against GT-1a and mutant variants.

To elucidate the causes of the loss of potency of WK-23 and WK-25, structural studies using X-ray crystallography that focus on these PIs in complex with both GT-1a and D168A proteases could inevitably lead to design of more potent inhibitors. Mapping which areas of the inhibitors protrude outside of the substrate envelope could show which parts of the inhibitor are the cause of the reduced potency in the D168A variants and in turn predict areas of concern that may confer drug resistance in other mutants, knowing this would refine the design of inhibitors moving forward.

6 REFERENCES

1. Alter, M. J. (2007). Epidemiology of hepatitis C virus infection. *World Journal of gastroenterology*, *13*(17), 2436.

2. Bartenschlager, R., Lohmann, V., & Penin, F. (2013). The molecular and structural basis of advanced antiviral therapy for hepatitis C virus infection.*Nature Reviews Microbiology*, *11*(7), 482-496.

3. Kwong, A. D. (2014). The HCV revolution did not happen overnight. *ACS medicinal chemistry letters*, *5*(3), 214-220.

4. Planas, R., Ballesté, B., Álvarez, M. A., Rivera, M., Montoliu, S., Galeras, J. A., ... & Solà, R. (2004). Natural history of decompensated hepatitis C virus-related cirrhosis. A study of 200 patients. *Journal of hepatology*, *40*(5), 823-830.

5. Poordad, F., & Dieterich, D. (2012). Treating hepatitis C: current standard of care and emerging direct-acting antiviral agents. *Journal of viral hepatitis*,*19*(7), 449-464.

6. Ohno, O., Mizokami, M., Wu, R. R., Saleh, M. G., Ohba, K. I., Orito, E., ... & Lau, J. Y. (1997). New hepatitis C virus (HCV) genotyping system that allows for identification of HCV genotypes 1a, 1b, 2a, 2b, 3a, 3b, 4, 5a, and 6a.*Journal of clinical microbiology*, *35*(1), 201-207.

7. Mabee, C. L., Crippin, J. S., & Lee, W. M. (1998). Review article: interferon and hepatitis C--factors predicting therapeutic outcome. *Alimentary pharmacology & therapeutics*, *12*(6), 509-518.

8. Okanoue, T., Sakamoto, S., Itoh, Y., Minami, M., Yasui, K., Sakamoto, M., ... & Sawa, Y. (1996). Side effects of high-dose interferon therapy for chronic hepatitis C. *Journal of hepatology*, *25*(3), 283-291.

9. Ortega-Prieto, A. M., Sheldon, J., Grande-Pérez, A., Tejero, H., Gregori, J., Quer, J., ... & Perales, C. (2013). Extinction of hepatitis C virus by ribavirin in hepatoma cells involves lethal mutagenesis. *PloS one*, *8*(8), e71039.

10. McHutchison, J. G., Gordon, S. C., Schiff, E. R., Shiffman, M. L., Lee, W. M., Rustgi, V. K., ... & Albrecht, J. K. (1998). Interferon alfa-2b alone or in combination with ribavirin as initial treatment for chronic hepatitis C. *New England Journal of Medicine*, *339*(21), 1485-1492.

11. Glue, P., Fang, J. W., Rouzier-Panis, R., Raffanel, C., Sabo, R., Gupta, S. K., ... & Jacobs, S. (2000). Pegylated interferon-α2b: Pharmacokinetics, pharmacodynamics, safety, and preliminary efficacy data. *Clinical Pharmacology & Therapeutics*, *68*(5), 556-567.

12. Manns, M. P., McHutchison, J. G., Gordon, S. C., Rustgi, V. K., Shiffman, M., Reindollar, R., ... & Group, I. H. I. T. (2001). Peginterferon alfa-2b plus ribavirin compared with interferon alfa-2b plus ribavirin for initial treatment of chronic hepatitis C: a randomised trial. *The Lancet*, *358*(9286), 958-965.

13. Pawlotsky, J. M. (2011). Treatment failure and resistance with direct-acting antiviral drugs against hepatitis C virus. *Hepatology*, *53*(5), 1742-1751.

14. McCauley, J. A., & Rudd, M. T. (2016). Hepatitis C virus NS3/4a protease inhibitors. *Current Opinion in Pharmacology*, *30*, 84-92.

15. Harper, S., McCauley, J. A., Rudd, M. T., Ferrara, M., DiFilippo, M., Crescenzi, B., ... & Romano, J. J. (2012). Discovery of MK-5172, a macrocyclic hepatitis C virus NS3/4a protease inhibitor. *ACS medicinal chemistry letters*, *3*(4), 332-336.

16. Bartels, D. J., Sullivan, J. C., Zhang, E. Z., Tigges, A. M., Dorrian, J. L., De Meyer, S., ... & Kieffer, T. L. (2012). HCV variants with decreased sensitivity to direct acting antivirals were rarely observed in DAA-naïve patients prior to treatment. *Journal of virology*, JVI-02294.

17. Romano, K. P., Ali, A., Aydin, C., Soumana, D., Özen, A., Deveau, L. M., ... & Huang, W. (2012). The molecular basis of drug resistance against hepatitis C virus NS3/4A protease inhibitors. *PLoS Pathog*, *8*(7), e1002832.

18. Soumana, D. I., Kurt Yilmaz, N., Prachanronarong, K. L., Aydin, C., Ali, A., & Schiffer, C. A. (2016). Structural and Thermodynamic Effects of Macrocyclization in HCV NS3/4A Inhibitor MK-5172. *ACS chemical biology*,*11*(4), 900-909.

19. Ali, A., Aydin, C., Gildemeister, R., Romano, K. P., Cao, H., Özen, A., ... & Schiffer, C. A. (2013). Evaluating the role of macrocycles in the susceptibility of hepatitis C virus NS3/4A protease inhibitors to drug resistance. *ACS chemical biology*, *8*(7), 1469-1478.

20. Copeland, R. A. (2013). *Evaluation of enzyme inhibitors in drug discovery: a guide for medicinal chemists and pharmacologists*. John Wiley & Sons.